

## FEEDBACK PROCESSES IN THE EARLY UNIVERSE

A. Ferrara<sup>1</sup>, B. Ciardi<sup>2</sup>, S. Marri<sup>3</sup> and P. Todini<sup>2</sup>

<sup>1</sup>Osservatorio Astrofisico di Arcetri, Firenze, Italy

<sup>2</sup>Max-Planck-Institut für Astrophysik, Garching, Germany

<sup>3</sup>Dipartimento di Astronomia, Università di Firenze, Italy

### ABSTRACT

Feedback effects due to massive stars and supernovae in the first objects are shown to strongly regulate both galaxy formation/evolution and the reionization process. Here we review the most important ones in some detail. We discuss how Type II supernovae can be used as tracers of the first objects and detected with NGST, for which we predict supernova number counts including the effects of gravitational lensing. Preliminary results on the formation of dust in the ejecta of supernovae of primordial composition are also presented. We finally turn to the consideration of the process of inhomogeneous reionization due to primordial stellar sources by means of high resolution numerical simulations, allowing for a self-consistent treatment of the above feedback processes. These simulations allow us to draw conclusions on the evolution and epoch of reionization and about the fate of reionizing objects. We conclude that a large fraction ( $\approx 99\%$ ) of collapsed objects must be dark at redshift around eight.

$\approx 10^{-7}$  at redshifts  $\gtrsim 400$  via the  $\text{H}_2^+$  formation channel. At redshifts  $\lesssim 110$ , when the Cosmic Microwave Background radiation (CMB) intensity becomes weak enough to allow for significant formation of  $\text{H}^-$  ions, a primordial fraction of  $f_{\text{H}_2} \approx 2 \times 10^{-6}$  (Galli & Palla 1998) is produced for model universes that satisfy the standard primordial nucleosynthesis constrain  $\Omega_b h^2 = 0.0125$  (Copi, Schramm & Turner 1995), where  $\Omega_b$  is the baryon density parameter and  $H_0 = 100h \text{ km s}^{-1} \text{ Mpc}^{-1}$  is the Hubble constant. This primordial fraction is usually lower than the one required for the formation of Pop III objects, but during the collapse phase the molecular hydrogen content can reach high enough values to trigger star formation. On the other hand, objects with virial temperatures (or masses) above that required for the hydrogen Ly $\alpha$  line cooling to be efficient, do not rely on  $\text{H}_2$  cooling to ignite internal star formation. Thus, the fate of a virialized lump depends crucially on its ability to rapidly increase its  $\text{H}_2$  content during the collapse phase. Tegmark *et al.* (1997) have addressed this question in great detail by calculating the evolution of the  $\text{H}_2$  abundance for different halo masses and initial conditions for a standard CDM cosmology. They conclude that if the prevailing conditions are such that a molecular hydrogen fraction of order of  $f_{\text{H}_2} \approx 5 \times 10^{-4}$  is produced during the collapse, then the lump will cool, fragment and eventually form stars. This criterion is met only by larger halos implying that for each virialization redshift there will exist some critical mass,  $M_{\text{crit}}$ , such that protogalaxies with total mass  $M > M_{\text{crit}}$  will be able to form stars and those with  $M < M_{\text{crit}}$  will fail. As an example, a  $3\sigma$  fluctuation of a Cold Dark Matter primordial spectrum, has  $M_{\text{crit}} \approx 10^6 M_\odot$  and collapses at  $z \approx 30$ .

### 1. THE FIRST OBJECTS

As the temperature of the cosmic bath decreases, atoms start to recombine and therefore decouple from CMB radiation at redshift  $\approx 1100$ . The baryonic Jeans mass after this event is given by (assuming  $\Omega = 1$ )

$$M_j \simeq 6 \times 10^4 \left( \frac{1+z}{30} \right)^{-3/2} \left( \frac{T}{500\text{K}} \right)^{3/2} \Omega_b M_\odot, \quad (1)$$

where  $T$  is the gas temperature and  $\Omega_b$  the baryon density parameter. Masses larger than  $M_j$  are gravitationally unstable and should, in principle, collapse. However, in order for the actual collapse to occur a more severe condition must be satisfied, *i.e.* that the cooling time of the gas is shorter than the Hubble time at that epoch. In fact, radiative losses provide the only way for the gas to lose pressure and to settle down in the potential well of the dark matter halo. Since the virial temperature corresponding to the masses of the first objects (PopIII) is typically  $\lesssim 8000 \text{ K}$ , cooling by hydrogen Ly $\alpha$  excitation is strongly quenched, and the only viable coolant in a primordial H-He plasma is molecular hydrogen.  $\text{H}_2$  is produced during the recombination phase, but its relic abundance is very small. Primordial  $\text{H}_2$  forms with a fractional abundance of

The first objects affect the subsequent galaxy formation, reionization and metal enrichment of the universe through their feedback effects. Generally speaking, two types of feedback, *radiative* and *stellar*, can be at work. They are related to the ionizing/  $\text{H}_2$  -photodissociating radiation and mechanical energy input from massive stars and supernovae, respectively. We discuss them in detail in the following.

### 2. RADIATIVE FEEDBACK

As stars are formed inside the first collapsed objects, their ionizing radiation produces HII regions in the surround-

ing IGM, thus triggering the reionization of the universe. In addition, their UV photons start to photodissociate  $\text{H}_2$  molecules in the neighbor objects. We have seen that  $\text{H}_2$  is a crucial species for the cooling to occur, and the lack of it might prevent the collapse of small protogalaxies. This process is known as *radiative feedback*. Particularly relevant is the soft UV background in the LW bands, as by dissociating the  $\text{H}_2$ , it could influence the star formation history of other small objects preventing their cooling.

Ciardi, Ferrara & Abel (2000) have shown that the UV flux from these objects results in a soft (Lyman – Werner band) UV background (SUVB),  $J_{LW}$ , whose intensity (and hence radiative feedback efficiency) depends on redshift. At high redshift the radiative feedback can be induced also by the direct dissociating flux from a nearby object. In practice, two different situations can occur: i) the collapsing object is outside the dissociated spheres produced by preexistent objects: then its formation could be affected only by the SUVB ( $J_{LW,b}$ ), as by construction the direct flux ( $J_{LW,d}$ ) can only dissociate molecular hydrogen on time scales shorter than the Hubble time inside this region; ii) the collapsing object is located inside the dissociation sphere of a previously collapsed object: the actual dissociating flux in this case is essentially given by  $J_{LW,max} = (J_{LW,b} + J_{LW,d})$ . It is thus assumed that, given a forming Pop III, if the incident dissociating flux ( $J_{LW,b}$  in the former case,  $J_{LW,max}$  in the latter) is higher than the minimum flux required for negative feedback ( $J_s$ ), the collapse of the object is halted. This implies the existence of a population of "dark objects" which were not able to produce stars and, hence, light.

To assess the minimum flux required at each redshift to drive the radiative feedback Ciardi *et al.* (2000, CFGJ) have performed non-equilibrium multifrequency radiative transfer calculations for a stellar spectrum (assuming a metallicity  $Z = 10^{-4}$ ) impinging onto a homogeneous gas layer, and studied the evolution of the following nine species: H,  $\text{H}^-$ ,  $\text{H}^+$ , He,  $\text{He}^+$ ,  $\text{He}^{++}$ ,  $\text{H}_2$ ,  $\text{H}_2^+$  and free electrons for a free fall time. We can then define the minimum total mass required for an object to self-shield from an external flux of intensity  $J_{s,0}$  at the Lyman limit, as  $M_{sh} = (4/3) \pi \langle \rho_h \rangle R_{sh}^3$ , where  $\langle \rho_h \rangle = \langle \rho_b \rangle \Omega_b^{-1}$  is the mean dark matter density of the halo in which the gas collapses;  $R_{sh}$  is the shielding radius beyond which molecular hydrogen is not photodissociated and allowing the collapse to take place on a free-fall time scale.

Values of  $M_{sh}$  for different values of  $J_{s,0}$  have been obtained at various redshifts (see Fig. 1) and will be then used in the reionization calculations discussed below. Protogalaxies with masses above  $M_H$  for which cooling is predominantly contributed by  $\text{Ly}\alpha$  line cooling will not be affected by the negative feedback studied here. The collapse of very small objects with mass  $< M_{crit}$  is on the other hand made impossible by the cooling time being longer than the Hubble time. Thus the only mass range in which negative feedback is important lies ap-

proximately in  $10^6 - 10^8 M_\odot$ , depending on redshift. In order for the negative feedback to be effective, fluxes of the order of  $10^{-24} - 10^{-23} \text{erg s}^{-1} \text{cm}^{-2} \text{Hz}^{-1} \text{sr}^{-1}$  are required. These fluxes are typically produced by a Pop III with baryonic mass  $10^5 M_{b,5} M_\odot$  at distances closer than  $\simeq 21 - 7 \times M_{b,5}^{1/2}$  kpc for the two above flux values, respectively, while the SUVB can reach an intensity in the above range only after  $z \approx 15$ . This suggests that at high  $z$  negative feedback is driven primarily by the direct irradiation from neighbor objects in regions of intense clustering, while only for  $z \leq 15$  the SUVB becomes dominant.

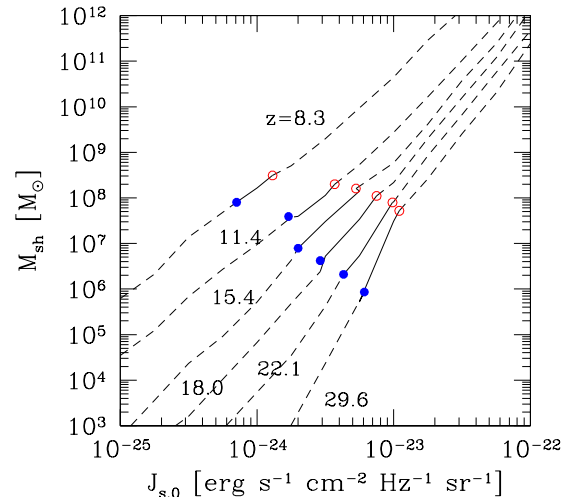


Figure 1. Minimum total mass for self-shielding from an external incident flux with intensity  $J_{s,0}$  at the Lyman limit. The curves are for different redshift: from the top to the bottom  $z = 8.3, 11.4, 15.4, 18.0, 22.1, 29.6$ . Circles show the value of  $M_H$  (open) and  $M_{crit}$  (filled). Radiative feedback works only in the solid portions of the curves.

### 3. STELLAR FEEDBACK

Once the first stars have formed in the host protogalaxy, they can deeply influence the subsequent star formation process through the effects of mass and energy deposition due to winds and supernova explosions. While low mass objects may experience a blowaway, expelling their entire gas content into the IGM and quenching star formation, larger objects may instead be able to at least partially retain their baryons. However, even in this case the blowout induces a decrease of the star formation rate due to the global heating and loss of the galactic ISM. These

two regimes are separated by a critical mass,  $M_{by}$  (CFGJ, Ferrara & Tolstoy 2000, MacLow & Ferrara 1999). For the relatively small objects present during the reionization epoch  $30 \gtrsim z \gtrsim 10$  the importance of these *stellar feedbacks* can hardly be overlooked. To understand the role of stellar feedback, let us consider a collapsed object with mass lower than  $M_{by}$ . Then the star formation is suddenly halted as the entire gas content is removed. In this case, the ionizing photon production will last only for a time interval of order  $t_{OB} \approx 10^7$  yr, the mean lifetime of the massive stars produced initially. After this phase, the ionized gas around the source will start to recombine at a fast rate as a result of the highly efficient high  $z$  Compton cooling, rapidly decreasing the temperature inside the ionized region. Due to the short lifetime and recombination time scales, these object will only produce transient HII regions which will rapidly disappear. In fact, the recombination time scale, when the Compton cooling is taken into account, is of order  $t_{rec} \approx (1-50) \times 10^6$  yr at redshift  $z \approx 30-10$ , respectively, and therefore much shorter than the corresponding Hubble time. The dissociating photon production will nevertheless continue for a longer time, due to the important contribution of long-lived intermediate mass stars formed in the same initial star formation burst. This, combined with the fact that there is no efficient mechanism available to re-form the destroyed  $H_2$  in the IGM analogous to H recombination, implies that the dissociation is not impeded by blowaway and the contribution from these small objects should be yet accounted for. However, this is not necessary. In fact, after blowaway,  $H_2$  is efficiently formed in the shocked IGM gas, cooling under non equilibrium conditions (Ferrara 1998). The final radius of the cooled shell behind which molecular hydrogen is formed by this process is:

$$R_s \simeq 224 M_{b,5}^{1/5} (1+z)^{-19/10} \text{ kpc}. \quad (2)$$

We notice that the formation process produces an amount of  $H_2$  roughly similar to the one destroyed by radiation (Ferrara 1998). A lower limit to the amount of molecular hydrogen produced in an explosion is readily found to be equal to  $M_{H_2}^+(z) \simeq (4\pi/3)\rho_b R_s^3 (2f)$  or

$$M_{H_2}^+(z) \simeq 102 f_{b,8}^{3/5} \Omega_{b,5} (1+z)^{-27/10} M_6^{1/5} f_6 h^{7/10} M_\odot. \quad (3)$$

The UV/ionizing radiation from Pop III massive stars previous to blow-away will produce both a HII region and a region of photodissociated intergalactic  $H_2$  (radius  $R_d$ ) in which the object is embedded. The radius  $R_d$  can be defined by requiring that the photodissociation timescale  $t_d$  is shorter than  $t_H$ . This condition yields the definition  $R_d = S_{LW}^{1/2} (1+z)^{-3/4} h^{-1/2}$ , where  $S_{LW} = \beta S_i(0)$  is the UV photon flux in the  $H_2$  Lyman-Werner (LW) bands (11.2–13.6 eV), assumed here to be proportional to the flux of Lyc photons,  $S_i(0)$ , just before the massive stars explode. The value of the constant  $\beta$  depends somewhat on the IMF and on the evolutionary stage of the stellar

cluster, but its value should be reasonably close to unity. We estimate  $S_i(0)$  to be

$$S_i(0) \simeq 10^{47} f_{uvpp,48} f_{esc,20} \Omega_{b,5} f_{b,8} M_5 \text{ s}^{-1}, \quad (4)$$

where  $f_{uvpp} = 48000 f_{uvpp,48}$  is the UV photon production per collapsed proton efficiency (Tegmark *et al.* 1994) and  $f_{esc} = 0.2 f_{esc,20}$  is the escape fraction of such photons. It is worth noticing that the latter quantity is rather uncertain. Recently, Dove, Shull & Ferrara (2000) have estimated the fraction of ionizing photons emitted by OB associations that escapes the H I disk of our Galaxy into the halo and intergalactic medium (IGM) by solving the time-dependent radiation transfer problem of stellar radiation through evolving superbubbles within a smoothly varying H I distribution. They find that the shells of the expanding superbubbles quickly trap or attenuate the ionizing flux, so that most of the escaping radiation escapes shortly after the formation of the superbubble. Superbubbles of large associations can blow out of the H I disk and form dynamic chimneys, which allow the ionizing radiation to escape the H I disk directly. However, blowout occurs when the ionizing photon luminosity has dropped well below the association's maximum luminosity. For a coeval star-formation history, the total fraction of Lyman Continuum photons that escape both sides of the disk in the solar vicinity is  $f_{esc} \approx 0.15 \pm 0.05$ ; for a Gaussian star formation history,  $f_{esc} \approx 0.06 \pm 0.03$ .

With these assumptions, it follows that

$$R_d \simeq (\beta S_{47})^{1/2} (1+z)_{30}^{-3/4} h^{-1/2} \text{ kpc}, \quad (5)$$

where  $S_{47} = S_i(0)/10^{47} \text{ s}^{-1}$ . Thus, the ratio between the  $H_2$  mass produced and destroyed by Pop IIIs is

$$\frac{M_{H_2}^+(z)}{M_{H_2}^-(z)} = \left( \frac{f}{f_{IGM}} \right) \left[ \frac{R_s}{R_d} \right]^3. \quad (6)$$

The previous relation is graphically displayed in Fig. 2 along with the values of  $R_s$  and  $R_d$ . From that plot we see that objects of total mass  $M_5 = 10$  produce more  $H_2$  than they destroy for  $z \lesssim 25$ ; larger objects ( $M_5 = 100$ ) provide a similar positive feedback only for  $z \lesssim 15$ , since they are characterized by a higher  $R_d/R_s$  ratio. However, since in a hierarchical model larger masses form later, even for these objects the overall effect should be a net  $H_2$  production.

As inside  $R_s$   $H_2$  is re-formed, the net effect on the destruction of intergalactic  $H_2$  of blown away objects is negligible (if not positive) and we can safely neglect them in the subsequent calculations.

In conclusion, low mass objects with mass  $< M_{by}$  produce ionization regions which last only for a recombination time; larger objects can survive but their star formation ability is impaired by ISM loss/heating. The detailed derivation of  $M_{by}$  can be found in CFGJ.

#### 4. EVOLUTIONARY TRACKS DUE TO FEEDBACKS

Fig. 3 illustrates all possible evolutionary tracks and final fates of primordial objects, together with the mass scales

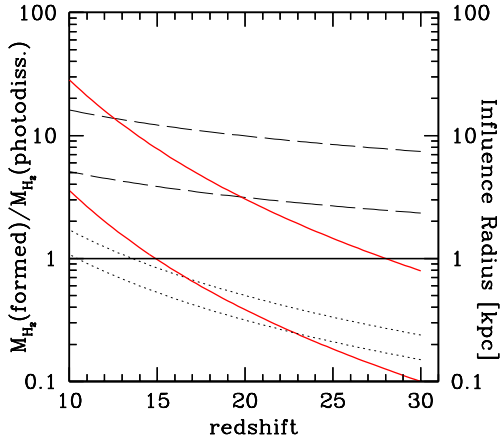


Figure 2. Ratio between the  $\text{H}_2$  mass formed and destroyed by a Pop III object as a function of the SNII explosion redshift (solid lines); values larger than one for the ratio define the epochs where Pop IIIs have a positive feedback on galaxy formation. Also shown are the shell (proper) radius at cooling,  $R_s$  (dotted), and the photodissociation (proper) radius,  $R_d$  (dashed). The upper set of curves refers to objects of mass  $M = 10^6 M_\odot$ , whereas the bottom one corresponds to larger objects,  $M = 10^7 M_\odot$ .

determined by the various physical processes and feedbacks. We recall that there are four critical mass scales in the problem: (i)  $M_{crit}$ , the minimum mass for an object to be able to cool in a Hubble time; (ii)  $M_H$ , the critical mass for which hydrogen Ly $\alpha$  line cooling is dominant; (iii)  $M_{sh}$ , the characteristic mass above which the object is self-shielded, and (iv)  $M_{by}$  the characteristic mass for stellar feedback, below which blowaway can not be avoided. Starting from a virialized dark matter halo, condition (i) produces the first branching, and objects failing to satisfy it will not collapse and form only a negligible amount of stars. In the following, we will refer to these objects as *dark objects*. Protogalaxies with masses in the range  $M_{crit} < M < M_H$  are then subject to the effect of radiative feedback, which could either impede the collapse of those of them with mass  $M < M_{sh}$ , thus contributing to the class of dark objects, or allow the collapse of the remaining ones ( $M > M_{sh}$ ) to join those with  $M > M_H$  in the class of *luminous objects*. This is the class of objects that convert a considerable fraction of their baryons

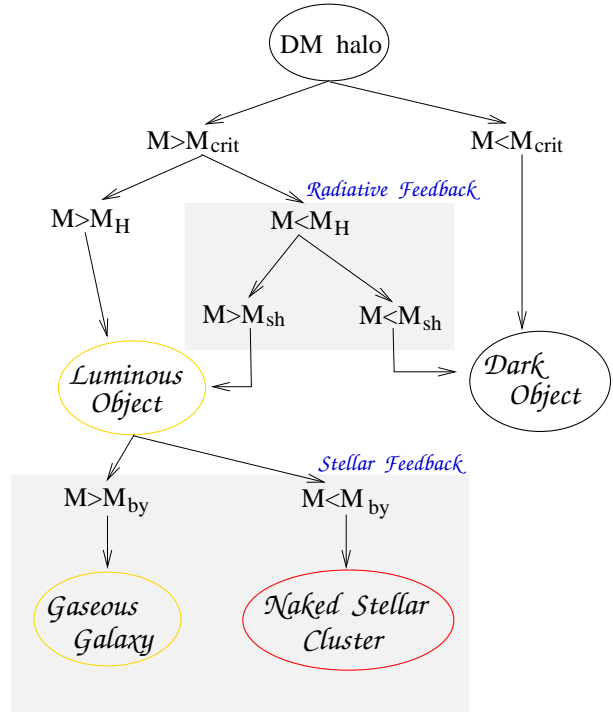


Figure 3. Possible evolutionary tracks of objects as determined by the processes and feedbacks discussed in this paper

in stars. Stellar feedback causes the final bifurcation by inducing a blowaway of the baryons contained in luminous objects with mass  $M < M_{by}$ ; this separates the class in two subclasses, namely “normal” galaxies (although of masses comparable to present day dwarfs) that we dub *gaseous galaxies* and tiny stellar aggregates with negligible traces (if any) of gas to which consequently we will refer to as *naked stellar clusters*.

## 5. DETECTING POPIII OBJECTS

Before we proceed to show how the reionization of the universe is regulated by stellar feedbacks, we briefly discuss possible strategies to observe PopIII objects. Given their small mass, these objects are likely to be faint: for a reasonable mass-to-light ratio for young galaxies  $\approx 0.1$ , their bolometric luminosity is  $\approx 2 \times 10^{40} \text{ erg s}^{-1}$ . A Type II SN is typically one hundred times brighter. Thus, for periods even longer than a year (taking into account the time stretching  $\propto (1+z)$  of the light curve) the SNII outshines its host galaxy. Since Type II SNe originate from massive stars, a necessary requirement is that the (unknown) IMF of these objects is flat enough to extend into this regime. Clearly, this condition is satisfied in the local universe, but it is not necessarily so in the conditions prevailing when the universe was young. Nevertheless, it is intriguing to speculate about the observational perspectives to detect very high  $z$  SNe, a possibility to which our hopes to in-

investigate directly the primeval star/galaxy formation are closely tied.

The advances in technology are making available a new generation of instruments, some already at work and some in an advanced design phase, which will dramatically increase our observational capabilities. As representative of such class, we will focus on a particular instrument, namely the Next Generation Space Telescope (NGST). In the following we will try to quantify the expectations for the detection of high  $z$  SNe. In addition to what we can learn on the formation of the first objects, Pop III SNII can provide crucial information on cosmological models due to their different predictions concerning the gravitational lensing magnification patterns by the intervening matter in the universe. The gravitational amplification might affect the SNII number counts and should be therefore properly taken into account (Marri & Ferrara 1998). As an example, taken from the study of Marri, Ferrara & Pozzetti (2000), we show the magnification map for the SCDM model for a source located at redshift 10 in Fig. 4. Fig. 5 shows the differential SNII counts [0.5 mag/ yr/

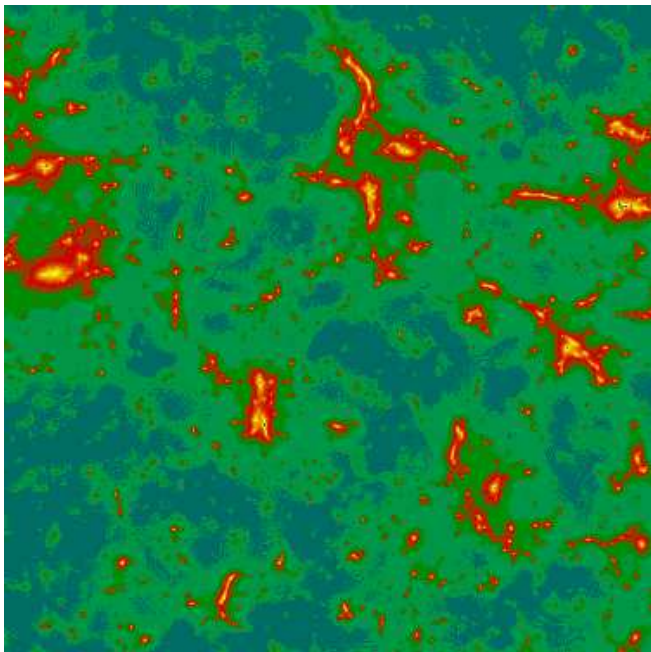


Figure 4. Magnification map for a SCDM model ( $4' \times 4'$ , corresponding to a NGST field) for a source located at  $z = 10$ . The magnification range is 0.7-50.

0.44 deg<sup>2</sup>] as a function of AB magnitude. The four panels contain the curves for the SCDM and LCDM models and for  $J$ ,  $K$ ,  $L$ , and  $M$  bands, both including or neglecting the effects of GL. For comparison, we plotted the NGST magnitude limit  $AB = 31.4$  (vertical line). This is calculated by assuming a constant limiting flux  $\mathcal{F}_{NGST} = 10$  nJy in the wavelength range  $1-5\mu\text{m}$  (*i.e.*  $J-M$  bands). This can

be achieved, for a 8-m (10-m) mirror size and a  $S/N=5$ , in about  $2.6 \times 10^4$  s ( $1.1 \times 10^4$  s)<sup>1</sup>. Thus, NGST should be able to reach the peak of expected SNII count distribution, which is located at  $AB \approx 30 - 31$  for SCDM and  $AB \approx 31 - 32$  for LCDM (depending on the wavelength band). The differences among the various bands are not particularly pronounced, although  $J$  and  $K$  bands present a larger number of luminous ( $AB \lesssim 27$ ) sources, and therefore they might be more suitable for the experiment. Furthermore, we point out that in the  $L$  and  $M$  bands NGST, with the current magnitude limit, will not be able to reach the peak of expected SNII count distribution in the LCDM model.

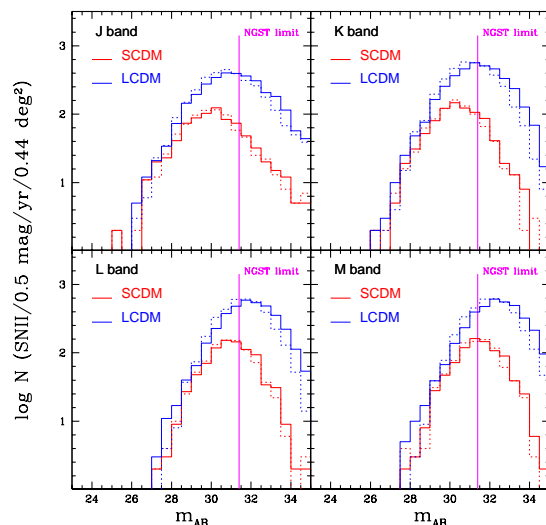


Figure 5. Differential number counts for the two cosmological models considered (thick solid line: SCDM, thin solid line: LCDM) as a function of apparent AB magnitude in  $J, K, L, M$  bands. Also shown is the NGST limiting magnitude. Dashed curves neglect lensing magnification.

## 6. MORE FEEDBACK FROM DUST FORMATION

In addition to the above mentioned feedback effects, SNII can also initiate molecular hydrogen formation on dust grain surfaces rather than in the gas phase, a more standard process in present day galactic environments. At high redshift Type II SNe are the only possible sources of dust, due to the short age of the universe and the long evolutionary timescales characterizing more conventional dust sources, as for example evolved stars. A detailed nucleation study of dust formation in the ejecta of Type II SNe

<sup>1</sup> This result has been obtained using the NGST Exposure Time Calculator, available at <http://augusta.stsci.edu>

whose initial chemical composition is primordial has been very recently carried on (Todini & Ferrara, in preparation). This case is suitable for the study of the very first SNII, as those originating in PopIII objects. From this study we have been able to derive several important properties characterizing the first solid particles produced in the universe, as for example the total dust mass produced, the dust composition and the grain size distribution. Preliminary results show that in the range of SNII masses considered,  $M_{SN} = 12 - 40M_{\odot}$ , typically  $0.1 M_{\odot}$  of dust is produced. SNII towards the low end of the mass distribution mostly produce silicate grains, whereas the most massive ones predominantly produce graphite grains; this fact is easy to understand in terms of the C/O ratio of their ejecta. The size distribution is approximated by a power-law for about two decades in radius (from  $\approx 1\text{\AA}$  to  $100\text{\AA}$ ) and shows a smooth cutoff beyond that grain radius. Thanks to these results we can now pose the following question: what is the minimum amount of dust required in order for the molecular hydrogen formation on grains to become competitive with the gas phase one? An order-of-magnitude answer can be obtained by comparing the two formation rates. At the low densities relevant here,  $\text{H}_2$  is formed in the gas phase mainly via the channel  $\text{H} + e^- \rightarrow \text{H}^- + h\nu$ , at rate  $k_8$  (the rate coefficient  $k_8$  is given in Abel *et al.* 1997); formation via the  $\text{H}_2^+$  channel, when included, is found to be negligible in our case. Therefore the formation rate in the gas phase is  $\mathcal{R} \simeq k_8 n_{\text{H}^-} n_{\text{H}}$ . The formation rate on grain surfaces is instead given by  $\mathcal{R}^d \simeq 0.5 \langle \gamma c_s \sigma \rangle n_d n_{\text{H}}$ , where  $\gamma$  is the sticking coefficient,  $c_s$  is the sound speed in the gas, and  $\sigma$  is the grain cross section. The equality between the two rates can be cast into the following form:  $\mathcal{D} = 0.1 \sqrt{T} x_e$ , where  $\mathcal{D}$  is the dust-to-gas ratio normalized to its Galactic value,  $T$  is the gas temperature and  $x_e$  the gas ionization fraction. For typical parameters of the PopIII objects,  $\text{H}_2$  production on dust grains becomes dominant once  $\mathcal{D}$  is larger than 5% of the local value. With the dust yields per SNII calculated above we then conclude that only about 15 SNII are required to enrich in dust to this level a primordial object. Clearly, early dust formation might play a role in the formation of the first generation of objects.

## 7. REIONIZATION HISTORY DRIVEN BY FEEDBACKS

In this final Section we summarize some of the results obtained by CFGJ on the evolution of inhomogeneous reionization, regulated by the feedback mechanisms introduced above and regulated by the molecular hydrogen network. For a broader presentation the reader is advised to refer to CFGJ. We have determined the spatial distribution of the ionizing sources from high resolution numerical N-body simulations within a periodic cube of comoving length  $L = 2.55h^{-1}$  Mpc for a critical density cold dark matter model ( $\Omega_0=1$ ,  $h=0.5$  with  $\sigma_8=0.6$  at  $z=0$ ). This allows us to describe the topology of the ionized and dis-

sociated regions at various cosmic epochs and derive the evolution of H, He, and  $\text{H}_2$  filling factors, soft UV background, cosmic star formation rate and the final fate of ionizing objects. There are three free parameters in the computation:  $f_b$ , the fraction of virialized baryons that is able to cool and become available to form stars,  $f_{\star}$  the star formation efficiency, and  $f_{esc}$  the photon escape fraction from the proto-galaxy. The variation of these free parameters defines four different runs A-D, whose parameter combination is shown in Tab. 1.

<i>RUN</i>	$f_b$	$f_{\star}$	$f_{esc}$
A	0.08	0.15	0.2
B	0.08	0.05	0.2
C	1.00	0.15	0.2
D	0.08	0.15	0.1

Table 1. Parameters of the calculation: fraction of virialized baryons that are able to cool and be available for star formation,  $f_b$ ; star formation efficiency,  $f_{\star}$ ; photon escape fraction,  $f_{esc}$ .

### 7.1. FILLING FACTORS

The filling factors of the dissociated  $\text{H}_2$  and ionized H and He are defined as the box volume fraction occupied by those species. The results are shown in Fig. 6, for the different runs. The intergalactic relic molecular hydrogen is found to be completely dissociated at very high redshift ( $z \approx 25$ ) independently of the parameters of the simulation. This descends from the fact that dissociation spheres are relatively large and overlap at early times. Ionization spheres are instead always smaller than dissociation ones and complete reionization occurs considerably later. Except for run C, when reionization occurs by  $z \approx 15$ , primordial galaxies are able to reionize the IGM at a redshift  $z \approx 10$ . The filling factor is approximately linearly proportional to the number of sources but has a stronger (cubic) dependence on the ionization sphere radius. Thus, although the number of (relatively small) luminous objects present increases with redshift, the filling factor is only boosted by the appearance of larger, and therefore more luminous, objects which can ionize more efficiently. The subsequent flattening at lower redshifts, is obviously due to the fact that when the volume fraction occupied by the ionized gas becomes close to unity most photons are preferentially used to sustain the reached ionization level rather than to create new ionized regions. The reionization is basically driven by objects collapsed through H line cooling, while small mass PopIII stars play only a minor role and even in the absence of a radiative negative feedback they would not be able to reionize the IGM. Note that only about 2% of the stars observed at



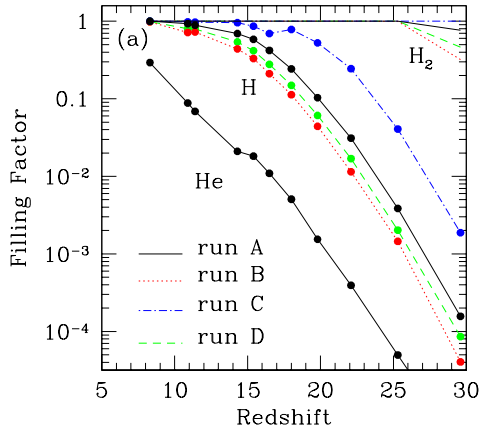


Figure 6. Evolution of the dissociated molecular hydrogen (upper set of lines), ionized atomic hydrogen (middle set) and doubly ionized helium (bottom line) filling factor as a function of redshift for different runs: A (solid line), B (dotted), C (dashed-dotted) and D (dashed). (b) same as (a) for runs: A (solid line), A1 (dotted) and A2 (dashed-dotted).

$z = 0$  is required to reionize the universe completely. This corresponds to an average IGM metallicity (assuming a Salpeter IMF) at redshift  $z \approx 10$  equal to  $\langle Z \rangle \approx 3 \times 10^{-4} Z_{\odot}$ .

## 7.2. WHAT IS THE FATE OF (RE)IONIZING SOURCES ?

The last point we make here concerns the final fate of the objects responsible for the reionization of the universe in terms of the evolutionary tracks introduced above; this discussion is summarized in Fig. 7. The straight lines represent, from the top to the bottom, the number of dark matter halos, dark objects, naked stellar clusters and gaseous galaxies, respectively. The dotted curve represents the number of luminous objects with large enough mass ( $M > M_H$ ) to make the H line cooling efficient and become insensitive to the negative feedback. We remind that the naked stellar clusters are the luminous objects with  $M < M_{by}$ , while the gaseous galaxies are the ones with  $M > M_{by}$ ; thus, the number of luminous objects present at a certain redshift is given by the sum of naked stellar clusters and gaseous galaxies. We first notice that the majority of the luminous objects that are able to form at high redshift will experience blowaway, becoming naked stellar clusters, while only a minor fraction, and only at  $z \lesssim 15$ , when larger objects start to form, will survive and become gaseous galaxies. An always increasing number of luminous objects is forming with decreasing redshift, until

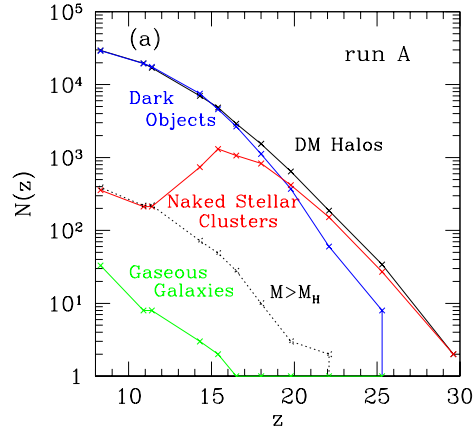


Figure 7. Number evolution of different objects in the simulation box for run A.

$z \approx 15$ , where a flattening is seen. This is due to the fact that the dark matter halo mass function is still dominated by small mass objects, but a large fraction of them cannot form due to the following combined effects: i) towards lower redshift the critical mass for the collapse ( $M_{crit}$ ) increases and fewer objects satisfy the condition  $M > M_{crit}$ ; ii) the radiative feedback due to either the direct dissociating flux or the SUVB increases at low redshift as the SUVB intensity reaches values significant for the negative feedback effect. When the number of luminous objects becomes dominated by objects with  $M > M_H$ , by  $z \approx 10$  the population of luminous objects grows again, basically because their formation is now unaffected by negative feedback. A steadily increasing number of objects is prevented from forming stars and remains dark; this population is about  $\approx 99\%$  of the total population of dark matter halos at  $z \approx 8$ . This is also due to the combined effect of points i) and ii) mentioned above. This population of halos which have failed to produce stars could be identified with the low mass tail distribution of the dark galaxies that reveal their presence through gravitational lensing of quasars. It has been argued in the recent literature that this population of dark galaxies outnumbers normal galaxies by a substantial amount, and Fig. 7 supports this view.

## 8. SUMMARY

We have discussed several feedback effects, mostly related to the presence of massive stars in early formed objects, and analyzed their impact on galaxy formation and reionization of the universe. A brief summary of the findings of

this paper (for a more detailed presentation see Ciardi *et al.* 2000) follows below:

- The first objects affect subsequent galaxy formation both via *radiative* and *stellar* feedbacks due to ionizing/ $H_2$  –photodissociating radiation and mechanical energy input due to massive stars and supernovae, respectively
- Molecular hydrogen is photodissociated but reformed behind SN shocks during blowaway/blowout events; dust can be formed in SNII ejecta, allowing for  $H_2$  formation on grain surfaces rather than in the gas phase.
- PopIII objects could be detected via their SNII with NGST; Up to  $z = 15$ , the (SCDM, LCDM) models predict a total number of (857, 3656) SNII/yr in 100 surveyed  $4' \times 4'$  fields of the *Next Generation Space Telescope*.
- Galaxies are able to reionize the neutral atomic hydrogen by a redshift  $z \approx 10$ , while molecular hydrogen is completely dissociated at very high redshift ( $z \approx 25$ ).
- IGM reionization is basically driven by objects collapsed through H line cooling ( $M > M_H$ ), while small mass objects ( $M < M_H$ ) play only a minor role and even in the absence of a radiative negative feedback they would not be able to reionize the IGM.
- A consistent fraction of halos is prevented from forming stars by either the condition  $M < M_{crit}$  or the effect of radiative feedback; this population of dark objects reaches  $\approx 99\%$  of the dark matter halo population at  $z \approx 8$ .

#### ACKNOWLEDGEMENTS

We would like to thank our collaborators T. Abel, J. Dove, F. Governato, A. Jenkins, M.-M. MacLow, L. Pozzetti, Y. Shchekinov and M. Shull for sharing their enthusiasm with us.

#### REFERENCES

- Abel, T., Anninos, P., Zhang, Y. & Norman, M. L. 1997, *NewA*, 2, 181
- Ciardi, B., Ferrara, A. & Abel, T. 2000, *ApJ*, in press
- Ciardi, B., Ferrara, A., Governato, F. & Jenkins, A. 2000, *MNRAS*, in press (astro-ph/9907189) (CFGJ)
- Copi, C. J., Schramm, D. N. & Turner, M. S. 1995, *Science*, 267, 192
- Dove, J., Shull, J.M. & Ferrara, A. 2000, *ApJ*, in press (astro-ph/9903331)
- Ferrara, A. 1998, *ApJ*, 499, L17
- Ferrara, A. & Tolstoy, E. 2000, *MNRAS*, in press (astro-ph/9905280)
- Galli, D. & Palla, F. 1998, *A&A*, 335, 403
- MacLow, M.-M. & Ferrara, A. 1999, *ApJ*, 513, 142
- Marri, S. & Ferrara, A. 1998, *ApJ*, 509, 43
- Marri, S., Ferrara, A. & Pozzetti, L. 2000, *MNRAS*, submitted